Light-induced activation and deactivation of bulk defects in boron-doped float-zone silicon

T. Niewelt,[1,2] M. Selinger,[1,2] N. E. Grant,[3] W. Kwapil,[1,2] J. D. Murphy,[3] and M. C. Schubert[1]
[1]*Fraunhofer Institute for Solar Energy Systems ISE, Heidenhofstraße 2, 79110 Freiburg, Germany*
[2]*Freiburg Materials Research Center FMF, Stefan-Meier-Straße 21, 79104 Freiburg, Germany*
[3]*School of Engineering, University of Warwick, Coventry CV4 7AL, United Kingdom*

(Received 6 March 2017; accepted 23 April 2017; published online 8 May 2017)

In this paper, we present new insight in the degradation and subsequent recovery of charge carrier lifetime upon light soaking at 75 °C observed in float-zone silicon wafers. Variations of doping type, dielectric passivation schemes and thermal treatments after layer deposition were performed. The degradation was only observed for p-type float-zone silicon wafers passivated with passivation schemes involving silicon nitride layers. An influence of thermal treatments after deposition was found. N-type wafers did not degrade independent of their passivation scheme. Room temperature re-passivation experiments showed the degradation to affect the wafer bulk, and photoluminescence studies demonstrated fine lateral striations of effective lifetime. We conclude that the degradation is caused by bulk defects that might be related to hydrogen complexes.
[http://dx.doi.org/10.1063/1.4983024]

I. INTRODUCTION

High purity float-zone (*FZ*) silicon wafers are commonly used for the development and optimisation of dielectric surface passivation layers intended for application in silicon photovoltaics and materials research. They may also be suitable for use as substrates in the highest efficiency silicon solar cells. The usually very high minority charge carrier lifetime due to the ultra-low concentration of impurities in this material allows extrapolation of surface recombination properties. The high electronic quality is also crucial for the quality control of, e.g., processes for high-efficiency solar cell concepts and measurement techniques. However, recent studies have revealed that even FZ wafers of high purity and electronic quality can be prone to the formation of recombination active defects during moderate temperature treatments, e.g., Ref. 1. Additional recombination activity in the wafer bulk hinders the optimization of surface passivation schemes and overlooking the underlying defects complicates their consideration.

Recently, Grant *et al.* and Sperber *et al.* have demonstrated the occurrence of bulk defect related recombination in p-type FZ silicon upon light soaking at elevated temperatures.[2,3] This effect was addressed as light-induced degradation (*LID*). It indicates formation or activation of defects in the FZ silicon wafer bulk under conditions that can become relevant for the application of solar cells depending on their location. The characterisation and stability testing of dielectric passivation schemes under such conditions is crucial for further device improvements. Therefore, investigation and understanding of the defect(s) are necessary. We have performed a more detailed study of the defect in question and find a strong correlation of the defect activation with temperature treatments and the application of silicon nitride layers, pointing towards an involvement of hydrogen from the nitride film in the process. Furthermore, we observed the absence of this additional recombination in n-type silicon, indicating the defect is either not present or not recombination active. The lateral distribution of the defect was studied and indications of an influence of the excess charge carrier concentration on the defect activation and deactivation were found.

II. EXPERIMENT

A. Sample preparation

Lifetime samples were prepared from high quality industrial 4 inch FZ silicon wafers of both p-type and n-type with a resistivity of 1 Ω · cm. The phosphorus doped n-type samples featured a nominal thickness of 200 μm, while the boron doped p-type samples were 250 μm thick. After wet chemical cleaning, the samples were subjected to a thermal pre-treatment in the form of an oxidation step at 1050 °C for 60 min in order to homogenize thermal history and avoid influence of the bulk defect class discussed by Grant *et al.*[1] We then address the wafer bulk as "*stabilized*" (e.g., in Fig. 1) as no changes of the wafer bulk lifetime due to temperature steps are expected after this treatment. Different dielectric layers and layer stacks were deposited on the full wafers to study their influence on the degradation effect. All samples were prepared symmetrically, i.e., with the same stack on both sides of the wafer. Aluminium oxide layers were deposited with either plasma-assisted atomic layer deposition (*PALD*) at 230 °C resulting in Al_2O_3 or via plasma-enhanced chemical vapour deposition (*PECVD*) at 300 °C resulting in AlO_x. The excellent surface passivation and stability to thermal treatments of such layers can be further improved by

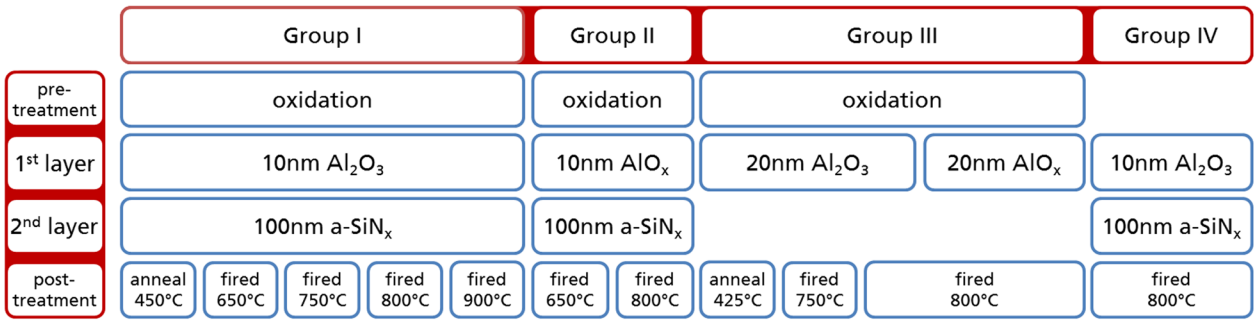

FIG. 1. Schematic overview of the investigated processes.

capping with an a-SiN_x layer deposited by PECVD.[4] This effect is presumed to arise at least partially from the introduction of hydrogen to the AlO_x/c-Si interface and the wafer bulk. Different thermal treatments were performed after deposition to activate the surface passivation and to vary the thermal history of the wafer bulk. Samples were either (1) "*annealed*" in air on a hotplate at 425 °C or 450 °C or (2) subjected to rapid thermal annealing in nitrogen gas in an RTP furnace. The rapid anneals will be addressed to as "*firing*" steps in this work to stress their similarity to contact firing processes in photovoltaic application. They featured four different set peak temperatures T_{set} (650 °C, 750 °C, 800 °C, and 900 °C) controlled by a pyrometer calibrated for the investigated samples via comparison to thermocouple measurements. We expect the actual sample temperatures to be in a range of $T_{set} \pm 15$ K. A measured temperature profile of the used process can be found in Ref. 5 (see Fig. 1, labelled "*RTP standard*"). The investigated combinations of layers, their thicknesses and thermal treatment are summarized in Fig. 1.

Photoluminescence imaging (PLI) was used to remove samples with process-induced damages (e.g., strong scratches) that could influence the lifetime measurement in the wafer centre.

B. Light soaking

After initial characterization of the effective lifetimes τ_{eff} via QSSPC (i.e., photoconductivity decay measurements in a Sinton Instruments Lifetime tester WCT-120) and lateral homogeneity via PLI, the samples were subjected to light soaking. They were placed on an actively temperature-controlled sample stage and illuminated by halogen lamps. The sample temperature was (75 ± 5) °C and the intensity was chosen to resemble the carrier generation of solar illumination (i.e., one *sun equivalent*). To monitor lifetime evolution, the samples were repeatedly removed from the sample stage and subjected to QSSPC measurements and PLI at one and 1/20 sun equivalents. The charge carrier lifetimes shown in this paper were extracted from measurements performed in the wafer centre evaluated at an excess charge carrier density Δn of 5×10^{15} cm^{-3} for both doping types. At this injection level, the passivation stacks used feature excellent passivation of both doping types.[6] Furthermore, this level is conveniently reachable in QSSPC measurements for the wide range of lifetimes that were observed in this study and provided reliable values of τ_{eff}. While intrinsic recombination due to radiative and Auger recombination is important at this injection, it is not rigorously limiting the effective lifetime and thus non-intrinsic recombination channels are still observable.

C. Room temperature re-passivation

In order to demonstrate the observed lifetime degradation to arise from recombination active bulk effects (i.e., not be due to surface passivation changes), three p-type samples at different stages of their progression were taken from the light soaking experiment and subjected to a room temperature re-passivation treatment. By this procedure, the dielectric passivation layers were chemically stripped from the silicon wafers, which were subsequently etched in 25% tetramethylammonium hydroxide (TMAH) for 10 min at ∼80 °C (removing ∼5 μm per side). Following the TMAH etch, the silicon wafers were dipped in 1% HF and subsequently cleaned in standard clean 2 (H_2O:H_2O_2:NH_4OH (1:1:5)) for 10 min at ∼75 °C. To complete the surface pre-treatment, the silicon samples were immersed (1 by 1) in 2% HF for 5 s and pulled dry from the HF solution. Directly following the HF dip, the samples were immersed in a non-aqueous solution of bis(trifluoromethane)sulfonimide (TFSI) dissolved in dichloroethane (2 mg/ml) for ∼60 s to achieve excellent surface passivation, as outlined in Refs. 7 and 8. With this passivation, further QSSPC and PLI characterization was performed. The purpose of this superacid passivation scheme was to re-passivate samples with a low surface recombination velocity to enable further QSSPC and PLI characterisation to be performed without exposing the samples to additional thermal processing.

III. RESULTS

QSSPC measurements of τ_{eff} in the initial state after thermal treatment demonstrated excellent passivation quality of most of the investigated dielectric layer systems. The achieved lifetime levels were affected by the suitability of the respective thermal treatment for the investigated layer system and the substrate doping type. Samples capped with a-SiN_x and treated at or below 800 °C consistently featured $\tau_{eff} > 1.25$ ms on p-type and >2 ms on n-type wafers at the investigated Δn of 5×10^{15} cm^{-3}. The higher lifetimes on n-type substrates are caused by the lower intrinsic bulk recombination rate (e.g., Ref. 9) and a slightly better achieved surface passivation quality. High temperature steps can cause a

deterioration of aluminium oxide based passivation stacks. However, throughout the study, we found that even effective surface recombination velocities in the range of up to 40 cm/s (e.g., due to 900 °C firing steps) were usually not hindering observation of the LID effect because the respective samples featured strong LID. A discussion of the achieved τ_{eff} on the sample set in terms of surface passivation quality can be found in Ref. 10.

In some of the samples, degradation of the measured effective lifetime upon light soaking at elevated temperature was observed. The degradation started immediately and was followed by a recovery to a stable state of high effective lifetimes, as observed by Sperber *et al.*[3] The lowest effective lifetimes were usually measured in an interval of 1–6 h of total light soaking duration and varied between samples of different preparations.

A. Influence of the doping type

In this study, we observed that effective lifetimes τ_{eff} of n-type samples remained stable within measurement uncertainty (or even improved) upon light soaking at 75 °C for multiple hours independent of the passivation stack and activation step used. By contrast, p-type samples processed alike consistently show LID. Exemplary lifetime measurements are shown in Fig. 2.

For the sake of clarity and brevity, no further lifetime measurements on n-type samples are shown in this work. For a more detailed study on the achieved passivation qualities on all investigated samples and their long-term stability to light-soaking at elevated temperatures, we refer to upcoming publications of the authors.[10,11]

B. Influence of thermal treatments

We observed the magnitude of degradation upon light soaking to depend on the process conditions to which the wafer was subjected. On samples with the same dielectric layer stack, we found a strong influence of the thermal treatment after deposition. Samples subjected to hotplate annealing (425 °C or 450 °C) or firing at 650 °C showed no or only slight degradation, while those fired with high peak temperatures degraded considerably. Stronger LID was found to correlate with higher peak temperature of the thermal treatment after deposition. Exemplary degradation curves are shown in Fig. 3.

We observed degradation and subsequent recovery upon light soaking on the samples that were not subjected to the thermal pre-treatment (i.e., the oxidation step to stabilize the wafer bulk, Group IV), as well. The degradation resembled corresponding samples from Group I that underwent the same treatment, but they featured lower τ_{eff} throughout the experiment.

C. Influence of dielectric layers

Samples passivated with 10 nm P-ALD Al_2O_3 and 100 nm PECVD a-SiN_x showed LID after being fired with a peak temperature of 800 °C manifested in a degradation and subsequent recovery of τ_{eff}. Furthermore, PL images in these samples featured characteristic rings, as will be discussed in Section III D. The same was found when an aluminium oxide layer was deposited by PECVD and capped with a 100 nm a-SiN_x layer, indicating that the deposition method of the aluminium oxide does not influence the defect.

Interestingly, however, we did not observe the characteristic dip in the measured τ_{eff} progression or clear signs of LID in the PL images of samples passivated with aluminium oxide but without an a-SiN_x capping. Such layers are less resilient to high temperature steps and many p-type samples after such treatment featured τ_{eff} values at a lower level than the curve shown in Fig. 4. It is therefore conceivable that the limitation imposed by the relatively low surface passivation

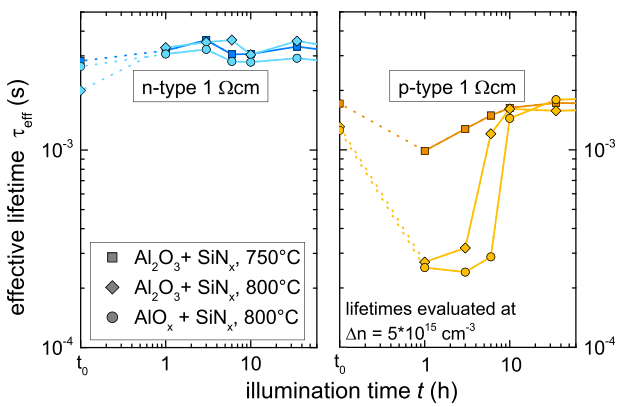

FIG. 2. Effective charge carrier lifetimes measured on lifetime samples from Groups I and II prepared on 1 Ω · cm n-type (left) and p-type (right) FZ silicon. The symbols denote transient and QSSPC lifetime measurements evaluated at $\Delta n = 5 \times 10^{15}$ cm^{-3} and the connections serve as guides-to-the-eye. The symbols indicate the processing sequence of passivation stack and firing temperature and apply to both doping types.

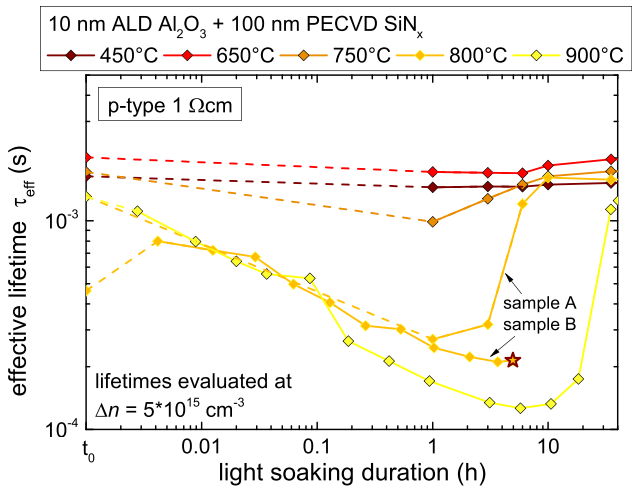

FIG. 3. Effective charge carrier lifetimes measured on Group I lifetime samples prepared on 1 Ω · cm p-type FZ silicon. All samples were passivated with the same dielectric layer system of 10 nm P-ALD Al_2O_3 and 100 nm PECVD a-SiN_x and only the thermal treatment after deposition was varied, as stated in the legend. The symbols denote transient QSSPC lifetime measurements evaluated at $\Delta n = 5 \times 10^{15}$ cm^{-3} and the connections serve as guides-to-the-eye. Dashed lines indicate the change between initial state and the first measurement during light-soaking. Samples A and B (both fired at 800 °C) underwent the superacid re-passivation treatment (see Section II C) in recovered and degraded states, respectively. The star symbol marks the stage at which sample B was studied. The results are presented in Fig. 5.

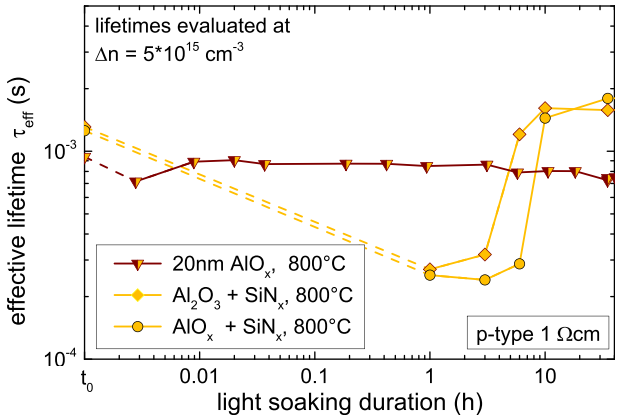

FIG. 4. Effective charge carrier lifetimes measured on lifetime samples from Groups I–III prepared on 1 Ω · cm p-type FZ silicon. The respective dielectric layer system and firing temperature are given in the legend. The symbols denote transient and QSSPC lifetime measurements evaluated at $\Delta n = 5 \times 10^{15}\,\mathrm{cm}^{-3}$ and the connections serve as guides-to-the-eye. Dashed lines indicate the change between initial state and the first measurement during light-soaking. Measurements on samples without a-SiN_x capping did not show definite signs of LID, as shown by the example curve (*triangles*).

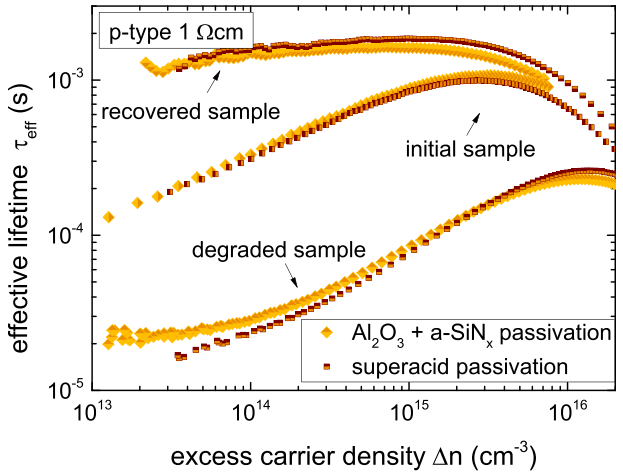

FIG. 5. Injection dependent lifetime curves of 1 Ω · cm p-type FZ wafers from Group I at different degradation stages before and after re-passivation. The samples were initially passivated with P-ALD Al_2O_3 and PECVD a-SiN_x and fired at 800 °C. The samples were measured before and after replacement of the dielectric passivation by room temperature superacid passivation. The agreement of the curves in degraded state demonstrates the LID effect to arise from bulk recombination, as opposed to changes in surface recombination. The curves in recovered state demonstrate the excellent passivation quality of the investigated layer stack even after extended light soaking (in this case 2200 h).

quality screens the LID effect. However, τ_{eff} in a-SiN_x capped affected sister samples in the study degraded severely and well below the lifetimes achieved on multiple single layer samples. Furthermore, characteristic structures were visible in PL images even on samples where little τ_{eff} degradation was detected by QSSPC. Thus, it appears that the LID either does not occur or drastically decreases upon omission of the a-SiN_x capping layer.

We achieved an excellent agreement of the measured τ_{eff} curves on the samples that underwent a room temperature superacid re-passivation treatment (as described in Section II C) with measurements before etching off the dielectric passivation. Both the injection level dependence and the absolute level of τ_{eff} measured with dielectric passivation were reproduced on samples in the initial, degraded and recovered states, as shown Fig. 5. Throughout the sample set, lifetime levels in the initial and recovered states were found to be similar for high injection conditions (see, e.g., Figs. 2–4). Curves measured on p-type samples prone to LID featured slightly rising injection dependence in low injection conditions, as shown in Figs. 5 and 6.

The samples whose τ_{eff} evolution is shown in Figs. 2–4 were processed together in the same batch. It should be noted that samples were processed alike but in later batches did not show the same magnitude of LID. However, only the magnitude in τ_{eff} varied, and all samples processed similar to those that exhibited degradation, featured the same characteristic τ_{eff} progression and lateral structures in PL imaging. Also, samples without a-SiN_x capping layer did not feature these LID characteristics.

D. Further investigations

While evaluation of τ_{eff} at fixed minority carrier density provides an easy measure to compare samples and follow their degradation, the actual recombination activity of defects manifests in the injection dependence of τ_{eff}. We found that samples showing LID in the time series evaluated at $\Delta n = 5 \times 10^{15}\,\mathrm{cm}^{-3}$ featured a characteristic injection dependent lifetime decrease. A brief analysis of the additional recombination in terms of a lifetime spectroscopy was performed. Injection-dependent QSSPC measurement curves at the time of minimum lifetime were corrected for surface recombination and potential bulk limitation not caused by LID. For that purpose, curves measured in initial or recovered state were inversely subtracted. The resulting curves of effective defect lifetimes τ_{def} were analysed via linearized lifetime spectroscopy (see Ref. 12). Good agreement with the data was achieved with the assumption of a deep defect

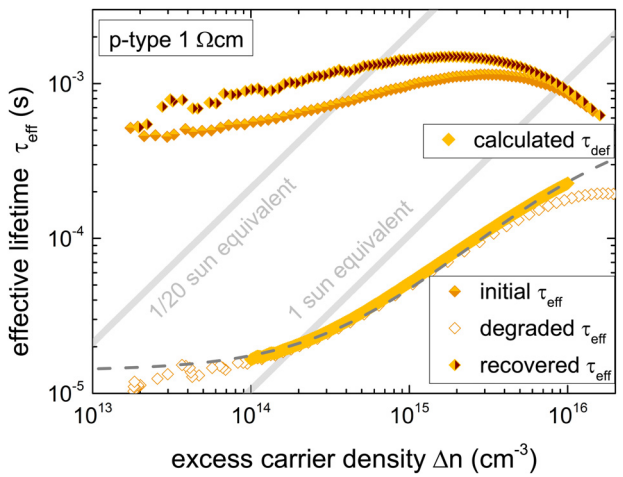

FIG. 6. Injection dependent lifetime curves measured on a sample from Group I at different stages of the light-soaking test. The sample was passivated with 10 nm P-ALD Al_2O_3 and 100 nm PECVD a-SiN_x and fired at 900 °C. The lines indicate the steady-state injection conditions at which images were taken in this experiment (some of which are shown in Figs. 7–9). The dashed line shows the lifetime limitation of a deep defect level with Q-factor of 40 according to Shockley-Read-Hall theory.

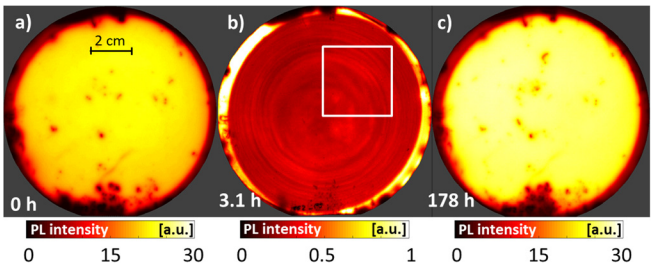

FIG. 7. PL images of a 1 Ω · cm p-type FZ sample from Group I featuring severe bulk lifetime degradation. The images are taken at 1 sun equivalent at different stages of LID indicated in the image. The sample was passivated with 10 nm P-ALD Al_2O_3, capped by 100 nm PECVD a-SiN_x and fired at 900 °C. The dark rim in (a) and (c) and bright rim in (b) originate from the a-SiN_x capping layer not covering the whole wafer. Note that image (b) has a very different color scale and features distinct striations of 5%–10%$_{rel}$. The white square in (b) indicates the wafer section further investigated in Fig. 8.

centre and an electron to hole capture coefficient ratio Q of 35 ± 10, as demonstrated in Fig. 6.

This capture coefficient asymmetry manifests in a steep change of τ_{def} (and thus τ_{eff} of affected samples) with minority charge carrier concentration. Therefore, steady-state illumination with homogeneous charge carrier generation rate creates distinct contrasts in the resulting Δn distribution, if lateral inhomogeneities in τ_{eff} occur. This was clearly observed in PL images of degrading samples that featured considerable lateral contrasts. An example is given in Fig. 7(b) for the sample shown in Fig. 6. Despite featuring a similar excess carrier concentration Δn, the PL image taken at 1/20 sun equivalent in recovered state (*not shown*) did not show striations.

During PLI characterization, we observed that the τ_{eff} recovery started first in the local regions of higher lifetime and spread from there. Such regions featured slightly higher PL intensity (indicating higher τ_{eff}) during degradation and showed rapid recovery after the global sample lifetime minimum was reached. An example is given in Fig. 8 for the part of the wafer marked in Fig. 7(b). The recovery of measured τ_{eff} was greatly affected by this local recovery due to the QSSPC averaging, while the majority of the wafer recovered by only a few percent, as demonstrated by PL imaging. Further light soaking steps showed the region of good lifetime to grow while the rest of the wafer recovered slower.

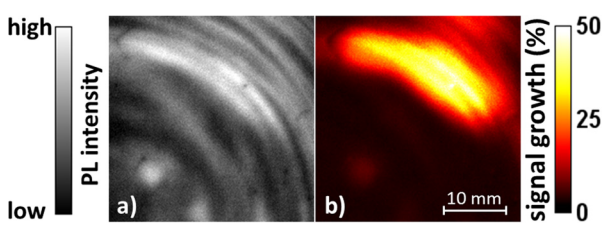

FIG. 8. Illustration of local sprouting of the lifetime recovery. (a) Detail view of the PL image shown in Fig. 7(b) featuring the characteristic circular striations and a local spot of higher lifetime. At this spot, the recovery started earlier than in the surrounding wafer, creating an expanding region of higher lifetime. (b) Illustration of the local PL signal growth of the spot upon light soaking at 75 °C for 460 min. Further light soaking steps caused further recovery accompanied by spreading of the resulting high lifetime region.

Another experimental finding is demonstrated in Fig. 9 in a magnification of the same region of a different wafer. Fig. 9 shows that the distribution and intensity of the PL signal changed upon intense laser illumination at room temperature. The wafer was placed on a cooled sample chuck at 25 °C and illuminated with an intensity of 2–3 sun equivalents for less than 5 s. This short treatment increased the τ_{eff} measured by QSSPC by 23%, which corresponds well with the measured PL intensity growth. It is interesting to note that this increase appears to correlate with the lateral PL signal distribution before the treatment.

IV. DISCUSSION

The observed lifetime degradation upon light–soaking at elevated temperatures in the studied samples corresponds well with the effect described by Sperber *et al.*[3] despite different base material. Besides the transitions reported by Sperber *et al.*, we observed lifetime recovery even at room temperature upon intense illumination. Re-passivation treatments of samples in initial, degraded and recovered state demonstrated the changes in τ_{eff} to arise from recombination in the wafer bulk, indicating activation and deactivation of recombination active defects. The capture coefficient ratio factor Q of 35 ± 10 we have determined on our samples agrees well with the results of Grant *et al.*[2] and is similar to the value reported by Sperber *et al.*[3] (their reported capture cross section ratios would resemble Q-factors of 30 and 24, respectively). The measurements render BO defects unlikely candidates for the defect, as the injection dependence of τ_{def} does not match the known BO defect species.[13] Also, the low oxygen content of the studied material $[O_i] < 10^{16}\,cm^{-3}$ (*supplier specification*) is by far not sufficient for a relevant influence of BO defects.[14] The found Q-factor is, however, similar to findings for a form of LID observed in multicrystalline silicon.[15] Recent results indicate the same effect to also occur in Czochralski grown silicon[16] under similar conditions to those tested in this work.

The injection dependence measured in initial state on samples prone to LID suggests those samples to be limited by defect recombination that vanishes upon LID recovery, as demonstrated in Figs. 5 and 6. We cannot yet distinguish whether the recombination is caused by an already activated

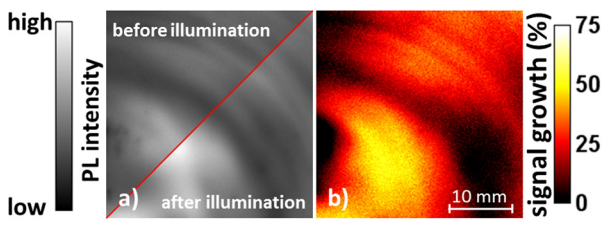

FIG. 9. Illustration of light-induced lifetime recovery at room temperature. (a) Detail of a PL image of an 800 °C fired sample from Group I after 5 h of light soaking (i.e., in a fully degraded state). The diagonal cut divides PL images taken at 1 sun equivalent before and after illumination of the sample with ~3 sun equivalents for several seconds. Surprisingly, this illumination created significant and permanent changes in the sample, as further manifested in a τ_{eff} change. (b) Illustration of the local PL signal growth at the image position. The average signal growth observed correlates well with the observed rise in τ_{eff}.

fraction of the defects responsible for LID or a precursor. The lower lifetime level and the injection dependent lifetime curves of the Group IV samples (*not shown*) indicate an additional lifetime limitation due to other recombination active defects. This is in accordance with the observations of Grant *et al.*[1] and indicates that the defects observed in this study are an additional defect species.

The n-type samples in this study exhibited stable τ_{eff} during light soaking at elevated temperature in the timeframe where p-type samples showed clear LID. According to Shockley-Read-Hall theory, the Q-factor we determined on p-type samples implies a weaker and likely injection-independent recombination limitation for n-type material. However, if we assume activation of similar defect concentrations in n-type material, an observable effect on lifetime would still be expected. The high and stable observed τ_{eff} level on n-type therefore indicates that the defect is either not formed/activated at all, in very different quantities or on a different timescale.

The timescale of participating processes can also be a crucial factor concerning the LID effect on p-type samples. The results indicate a strong influence of charge carrier injection on the observed lifetime recovery. The observed spreading of recovered spots indicates that out-diffusion of excess charge carriers from the more recovered spots supports the recovery of the vicinity and Fig. 9 even demonstrates rapid recovery at room temperature upon intense illumination. The results of Sperber *et al.* imply that carrier injection is also crucial for the degradation itself, as it does not occur—and is even reversible—through annealing in the dark. The resulting three state equilibrium of initial, degraded and recovered state discussed for LID in FZ by Sperber *et al.* is similar to the one for BO defects suggested by Herguth and Hahn.[17] Based on this model, the observed higher magnitude of degradation upon higher temperatures of processes after layer deposition could be caused by either an increased total concentration or a higher relative share of active defects due to retardation of the recovery reaction. At the current state, we cannot distinguish whether the observed magnitudes and the scattering thereof are related to a concentration variation or manifestation of a kinetic interaction. The samples from Group IV did not undergo the oxidation step bulk pretreatment exhibited similar degradation to sister samples that did. This indicates that the defects in question are not affected by the oxidation process.

The absence of lifetime degradation in the samples that did not feature the PECVD a-SiN_x capping layer can be considered an indication of involvement of hydrogen in the effect. Release of hydrogen from a-SiN_x layers to the AlO_x/c-Si interface and the silicon bulk during high temperature steps is strongly suspected, while long-ranged diffusion of other species during the short firing step appears unlikely. Besides the ability to passivate other defects, hydrogen can also cause or change the activity of recombination active defects.[18–20] Thus, an involvement of hydrogen in the effect is a likely explanation for the observed behaviour. An interpretation of the firing temperature dependence observed in this work would then be a higher total amount of hydrogen released into the silicon at higher peak temperatures of post-deposition treatments. Similar mechanisms are discussed for the influence of firing steps on the LID observed in multicrystalline silicon (e.g., Ref. 5) and the recovery of samples affected by BO degradation (e.g., Ref. 21).

At moderate temperatures, most hydrogen in p-type silicon is positively charged. Under illumination, a growing fraction of hydrogen atoms occupies a neutral state.[22] According to the model of Sun *et al.*, the charge state occupation of hydrogen in illuminated n-type resembles the situation in p-type silicon.[22] If the degradation is caused by formation of a coulomb bound complex of H with another constituent, this constituent should be or become negatively charged upon illumination in p-type but not in n-type silicon. The capture coefficient ratio Q we have determined indicates the resulting defect to be positively charged.

The lateral distribution of PL intensity observed in PLI and shown in Fig. 7(b) resembles patterns observed in PL-based dopant concentration imaging of FZ wafers (e.g., in Ref. 23). However, the observed distribution cannot be caused by mere doping concentration striations, as proven by two features shown in Figs. 6 and 7: (1) The excess carrier density Δn underlying Fig. 7(b) can be estimated with the curves in Fig. 6 to around $(2–5) \times 10^{15}\,cm^{-3}$ resembling a ratio $\Delta n/N_{dop}$ of about 0.3. It is shown in Appendix from the dependence of the PL intensity on charge carrier concentrations, $I_{PL} \propto n{\cdot}p$, that for such injection levels the relative variation in N_{dop} needs to be larger than observed intensity variations ΔI_{PL}, whereas relative variations in τ_{eff} may be smaller than observed ΔI_{PL}. In numbers, e.g., observed striations in I_{PL} of 5% would require variations of N_{dop} of 6.5%, whereas 4.0% variation in τ_{eff} could cause the same effect. Radial doping concentration variations in p-type FZ material are rather in a <5% range,[23] and thus the observed PL intensity variations of up to 10% are unlikely to be caused purely by doping variation. (2) As shown in Fig. 6, PL images in the recovered lifetime state but at lower illumination intensity (e.g., 1/20 sun equivalents) featured the similar Δn range but did not show any striations, indicating the actual N_{dop} variations to be small.

Therefore, we conclude that the concentration N_t of activated or formed defects responsible for the observed LID is not radially homogeneous but shows fine striations in a characteristic pattern. The fascinating resemblance of this defect distribution pattern to the doping striations found by Lim *et al.*[23] indicates that the concentration of the defect in question is related either to quantities affected by the same mechanism causing dopant concentration striations or to doping concentration itself. In the latter case, the observed ΔI_{PL} could be a superposition of ΔN_{dop} and ΔN_t. Either way, defect formation or activation could be related to an interaction with hydrogen followed by its detachment and binding in sinks or a reconfiguration of the defect that causes the lifetime recovery. The insights gathered from our experiments cannot yet confirm or discard whether the degradation is caused by the same defects that are responsible for LID of multicrystalline[15] and Czochralski grown silicon.[16]

It should be noted that the lateral inhomogeneities observed by PL imaging obstruct a detailed kinetic analysis of the measured progressions of τ_{eff} without an in-depth

analysis beyond the scope of this work. The presented values of τ_{eff} were measured with a Sinton Instruments WCT-120 Lifetime tester in the wafer centre and are therefore laterally averaged. This averaging could be assessed by taking the measurement mode (i.e., QSS and transient mode introducing different averaging functions, e.g., Ref. 24) and lateral sensitivity variations of the setup (see, e.g., Ref. 25) into account. However, the limited data set would still not allow quantitative kinetic evaluation, even if τ_{eff} averaging artefacts were corrected for. This is because PL imaging indicated a strong influence of the injection density on the process kinetics and local injection was not monitored in detail.

V. CONCLUSION

The effect of LID in FZ silicon upon light soaking at elevated temperatures was investigated on a sample set featuring a range of process variations common for photovoltaic and scientific applications. The effect was observed in a multitude of different p-type samples, while n-type samples appear to be unaffected. We observed a growing magnitude of the lifetime degradation with rising peak temperature of a short high temperature step performed after layer deposition. No fundamental differences were observed between samples featuring aluminium oxide layers deposited by ALD or PECVD when they were capped by an a-SiN_x layer deposited by PECVD to enhance thermal stability. However, omission of such protective layers significantly changed the reaction to light soaking, as no LID was observable on such samples. This indicates a contribution of the hydrogen released from such layers into the aluminium oxide layers and the silicon bulk to contribute to the effect.

From our experiments, the observed LID effect can be conclusively related to recombination activity in the silicon bulk. The observed lifetime degradation upon light soaking followed by complete recovery indicates that the underlying recombination active defects are activated and subsequently deactivated by the light soaking conditions. This agrees well with the observations of by Sperber *et al.*[3,26] on samples passivated only by a-SiN_x.

The observed characteristic pattern of PL intensity exhibits fine striations along the wafer diameter that resemble the oscillations of dopant concentrations observed by Lim *et al.*[23] and similar measurements we have performed. However, the contrasts in PL intensity exceed typical N_{dop} variations and thus indicate that the defect concentration distribution exhibits similar striations. This could be due to an involvement of dopant atoms in the recombination active defect.

QSSPC measurements revealed τ_{eff} as low as 30 μs at low Δn levels despite good surface passivation. The impact of the defect on the measured τ_{eff} is severely influenced by sample processing factors that are not yet understood and an influence of the testing conditions is expected. The analysed defect could thus affect a wide variety of scientific studies and applications of FZ silicon and should be investigated in more detail.

ACKNOWLEDGMENTS

This work was supported by the German Federal Ministry for Economic Affairs and Energy *BMWi* and by the industry partners within the research cluster SolarLIFE under Contract No. 0325763A. Work at the University of Warwick was supported by the EPSRC SuperSilicon PV project (Grant No. EP/M024911/1). The authors are responsible for the content.

APPENDIX: ESTIMATION OF PL CONTRASTS

The discussion mentions two theories on the origin of the observed variation ΔI_{PL} between two ROI 1 and 2:

First, a contrast originating from a variation of the doping concentration ΔN_{dop} with constant Δn,

$$\frac{\Delta I_{PL}}{I_{PL,1}} = \frac{\Delta n\left(N_{dop,2}+\Delta n\right) - \Delta n\left(N_{dop,1}+\Delta n\right)}{\Delta n\left(N_{dop,1}+\Delta n\right)} = \frac{N_{dop,2}-N_{dop,1}}{\left(N_{dop,1}+\Delta n\right)},$$

$$N_{dop,2} = N_{dop,1}\cdot\left(1+\left(1+\frac{\Delta n}{N_{dop,1}}\right)\cdot\frac{\Delta I_{PL}}{I_{PL,1}}\right).$$

For example, $\frac{\Delta I_{PL}}{I_{PL,1}} = 0.05$ and $\frac{\Delta n}{N_{dop,1}} = 0.3$ require $N_{dop,2} = 1.065\cdot N_{dop,1}$.

Second, a contrast arising from a variation in Δn caused by a difference in τ_{eff} for constant N_{dop},

$$\frac{\Delta I_{PL}}{I_{PL,1}} = \frac{\Delta n_2\left(N_{dop}+\Delta n_2\right) - \Delta n_1\left(N_{dop}+\Delta n_1\right)}{\Delta n_1\left(N_{dop}+\Delta n_1\right)} = \frac{\Delta n_2\left(N_{dop}+\Delta n_2\right)}{\Delta n_1\left(N_{dop}+\Delta n_1\right)} - 1,$$

$$\frac{\Delta n_2}{N_{dop}} + \left(\frac{\Delta n_2}{N_{dop}}\right)^2 = \left(1+\frac{\Delta I_{PL}}{I_{PL,1}}\right)\cdot\left(\frac{\Delta n_1}{N_{dop}} + \left(\frac{\Delta n_1}{N_{dop}}\right)^2\right),$$

or $\frac{\Delta n_2}{\Delta n_1} = \left(1+\frac{\Delta I_{PL}}{I_{PL,1}}\right)\cdot\left(\frac{N_{dop}+\Delta n_1}{N_{dop}+\Delta n_2}\right)$ with the last term being $\lesssim 1$.

For example, $\frac{\Delta I_{PL}}{I_{PL,1}} = 0.05$ and $\frac{\Delta n_1}{N_{dop}} = 0.3$ require $\frac{\Delta n_2}{N_{dop}} = 0.312$ resembling $\tau_{eff,2} = 1.04\cdot\tau_{eff,2}$.

[1]N. E. Grant, V. P. Markevich, J. Mullins, A. R. Peaker, F. Rougieux, and D. Macdonald, Phys. Status Solidi RRL **10**(6), 443–447 (2016).
[2]N. E. Grant, F. E. Rougieux, D. Macdonald, J. Bullock, and Y. Wan, J. Appl. Phys. **117**(5), 055711 (2015).
[3]D. Sperber, A. Herguth, and G. Hahn, Phys. Status Solidi RRL **11**(3), 1600408 (2017).
[4]A. Richter, J. Benick, M. Hermle, and S. W. Glunz, Phys. Status Solidi RRL **5**(5–6), 202–204 (2011).
[5]R. Eberle, W. Kwapil, F. Schindler, M. C. Schubert, and S. W. Glunz, Phys. Status Solidi RRL **10**(12), 861–865 (2016).
[6]G. Dingemans and W. M. M. Kessels, J. Vac. Sci. Technol., A **30**(4), 040802 (2012).
[7]J. Bullock, D. Kiriya, N. Grant, A. Azcatl, M. Hettick, T. Kho, P. Phang, H. C. Sio, D. Yan, D. Macdonald, M. A. Quevedo-Lopez, R. M. Wallace, A. Cuevas, and A. Javey, ACS Appl. Mater. Interfaces **8**(36), 24205–24211 (2016).
[8]N. E. Grant, T. Niewelt, N. R. Wilson, J. Bullock, M. Al-Amin, M. C. Schubert, A. C. van Veen, A. Javey, and J. D. Murphy, "Superacid-treated silicon wafers: Extending the limits of bulk and surface lifetimes for high efficiency photovoltaic devices" (submitted).

[9]A. Richter, S. W. Glunz, F. Werner, J. Schmidt, and A. Cuevas, Phys. Rev. B **86**(16), 165202 (2012).
[10]T. Niewelt, W. Kwapil, M. Selinger, A. Richter, and M. C. Schubert, "Long-term stability of Aluminium oxide based surface passivation schemes under illumination at elevated temperatures," IEEE J. Photovoltaics (submitted).
[11]T. Niewelt, W. Kwapil, M. Selinger, and M. C. Schubert, "Stability of AlOx surface passivation schemes under in-field application conditions," Energy Procedia (submitted).
[12]J. D. Murphy, K. Bothe, R. Krain, V. V. Voronkov, and R. J. Falster, J. Appl. Phys. **111**(11), 113709 (2012).
[13]T. Niewelt, J. Schön, W. Warta, S. W. Glunz, and M. C. Schubert, IEEE J. Photovoltaics **7**(1), 383–398 (2016).
[14]K. Bothe, R. Sinton, and J. Schmidt, Prog. Photovoltaics **13**, 287–296 (2005).
[15]D. Bredemeier, D. Walter, S. Herlufsen, and J. Schmidt, Energy Procedia **92**, 773–778 (2016).
[16]F. Fertig, R. Lantzsch, A. Mohr, M. Schaper, M. Bartzsch, D. Wissen, F. Kersten, A. Mette, S. Peters, A. Eidner, J. Cieslak, K. Duncker, M. Junghänel, E. Jarzembowksi, M. Kauert, B. Faulwetter-Quandt, D. Meißner, B. Reiche, S. Geißler, S. Hörnlein, C. Klenke, L. Niebergall, A. Schönmann, A. Weihrauch, F. Stenzel, A. Hofmann, T. Rudolph, A. Schwabedissen, M. Gundermann, M. Fischer, J. W. Müller, and D. J. W. Jeong, "Mass production of p-type Cz silicon solar cells approaching average stable conversion efficiencies of 22 %," Energy Procedia (submitted).
[17]A. Herguth and G. Hahn, J. Appl. Phys. **108**(11), 114509 (2010).
[18]A. R. Peaker, V. P. Markevich, B. Hamilton, G. Parada, A. Dudas, A. Pap, E. Don, B. Lim, J. Schmidt, L. Yu, Y. Yoon, and G. Rozgonyi, Phys. Status Solidi A **209**(10), 1884–1893 (2012).
[19]S. Leonard, V. P. Markevich, A. R. Peaker, B. Hamilton, and J. D. Murphy, Appl. Phys. Lett. **107**(3), 032103 (2015).
[20]W. Jost and J. Weber, Phys. Rev. B **54**(16), R11038–R11041 (1996).
[21]S. Wilking, J. Engelhardt, S. Ebert, C. Beckh, A. Herguth, and G. Hahn, in *28th European Photovoltaic Solar Energy Conference and Exhibition, Paris, France*, 2013, pp. 34–38.
[22]C. Sun, F. E. Rougieux, and D. Macdonald, J. Appl. Phys. **117**(4), 045702 (2015).
[23]S. Y. Lim, M. Forster, X. Zhang, J. Holtkamp, M. C. Schubert, A. Cuevas, and D. Macdonald, IEEE J. Photovoltaics **3**(2), 649–655 (2013).
[24]J. Giesecke, Ph.D. dissertation, University of Constance, 2014.
[25]J. A. Giesecke, M. C. Schubert, B. Michl, F. Schindler, and W. Warta, Sol. Energy Mater. Sol. Cells **95**(3), 1011–1018 (2011).
[26]D. Sperber, A. Heilemann, A. Herguth, and G. Hahn, IEEE J. Photovoltaics **7**(2), 463–470 (2017).